Empirical Modal and Theoretical Finite Element Analyses of Basketball-Rim Parameters versus Changes in Inflation Pressure

Daniel Winarski *, Kip P. Nygren , Tyson Winarski

Posted Date: 2 April 2025

doi: 10.20944/preprints202504.0177.v1

Keywords: modal analysis; finite element analysis; basketball; rim; eigenvector rotation; radial spring rate; modal damping ratios; correlation

 doi:10.20944/preprints202504.0177.v1

Article

Empirical Modal and Theoretical Finite Element Analyses of Basketball-Rim Parameters versus Changes in Inflation Pressure

Daniel Winarski [1,*], Kip P. Nygren [2] and Tyson Winarski [3]

[1] Independent Researcher, Tucson, AZ 85710 USA
[2] Independent Researcher, Wilmington, NC 28405, USA
[3] Sandra Day O'Conner College of Law, Phoenix Campus, Arizona State University, Phoenix, AZ 85004, USA
* Correspondence: winarskifirm@gmail.com

Abstract: The goal of this study was to quantify the sensitivity of the radial spring rate of a basketball, and the damping ratios of the first two modes of vibration of the basketball interacting with a Gared rim, to the change of inflation pressure. The chosen method of empirical modal analysis was impulse-response, where taps of an impact hammer provided the excitation and an accelerometer measured the response. The ANSYS 2025R1 Workbench modal analysis system was used to compliment the empirical modal analysis, by providing additional insight regarding the first two modes of vibration of the basketball-rim system. Our hypothesis was that the radial spring rate of the basketball would have a high positive correlation, and the damping ratios of the first two modes of vibration of the basketball and rim would have a high negative correlation, with respect to basketball inflation pressure. This study introduced studying the rotation of the modal eigenvectors with respect to the change of inflation pressure to better understand the physics of basketball-rim vibrations.

Keywords: modal analysis; finite element analysis; basketball; rim; eigenvector rotation; radial spring rate; modal damping ratios; correlation

1. Introduction

This study was inspired by the works of Okubo [1-6], and interactions with co-author Mont Hubbard, who analyzed the dynamics of basketball-rim interactions by using nonlinear ordinary differential equations to describe three components of ball angular velocity and contact point position on the toroidal rim. The rim and backboard were assumed to be rigid in this study. High speed video (500-1000 Hz) was used to capture actual basketball bounce tests to assess the radial spring rate and damping of a basketball. The inflation pressure P=8 psi was kept constant, whereas we varied the inflation pressure to see what sensitivity it had on the radial spring rate and damping ratio. We assumed that the rim was elastic, not rigid, and we applied impulse-response modal analysis rather than employ drop tests.

Other studies proved very useful. The impact studies of Tanaka, et-al., [7], Matsuda, et-al., [8], Takizawa, et-al., [9], and Yin, et-al., [10]. Tanaka used finite element analysis to model carbon-fibre reinforced golf clubs, specifically to study the effect torsional shaft stiffness had on golf ball impact. Matsuda used finite element analysis simulated the deformation of the string bed in a tennis racket due to a tennis ball. Via nonlinear finite element analysis, Takizawa concluded that the nonlinear mechanical properties of the polymer strings of the badminton racket made the calculated sweet-spot of the string planes smaller. Yin employed the finite element method to evaluate the von Mises stress distribution in the string-bed of a badminton racket upon the impact of the hemispherically-shaped nose of a shuttlecock. Nonuniform string tension, nonlinear friction between strings, and different impact locations were included in Yin's study.

 doi:10.20944/preprints202504.0177.v1

Javorksi, et-al., [11] first characterized the dynamic behavior of a ceiling-mounted basketball goal using an impact hammer and a fixed-location accelerometer, and then compared that empirical analysis to a theoretical finite element analysis. Empirical vibration measurements were taken at fourteen nodes, ten of which were on the frame supporting the basketball rim and backboard. Only four nodes were measured on the backboard, at the corners of the backboard, and none on the rim itself. Overall, 36 frequency response functions were measured, and this study concentrated mostly on structural vibrations between 2 and 10 Hz. Thus, this important study was focused more on the structural support of the backboard and rim rather than the elastic vibrations of the backboard and rim themselves.

The plate vibration studies by Nkounhawa, et-al., [12], Guguloth, et-al., [13], Irving [14], Dumond, et-al., [15], Anđelić, et-al., [16], and Geveci, et-al., [17] were all very helpful. Covill, et-al., [18] structural study gave additional insight.

2. Modal Analysis of Gared Rim in Isolation

The first analysis is that of one Gared rim in isolation [19]. Figure 1 shows the dimensions of this Gared Rim [19-20] and how it was mounted to a steel channel in lab D-18, Mahan Hall, at the United States Military Academy at West Point. A Brüel & Kjær 4393 Accelerometer [21] was mounted to outer end of the rim with beeswax. When used, pertubation mass *Mp* was also hung from the outer end of the rim.

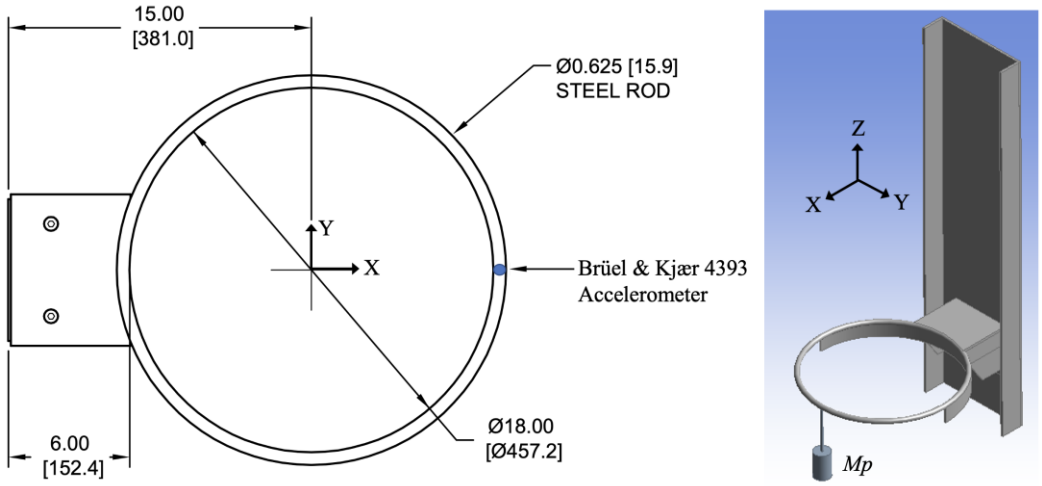

Figure 1. Dimensions of Gared rim and mounting onto a steel channel.

Figure 2 shows both a lumped spring-mass model and an finite-element model of the flexure of the Gared rim. The flexure displacement of the finite-element model is color coded, where the color red denotes maximum flexure displacement, followed by orange, yellow, green, cyan, to blue. Blue denoted minimum flexure displacement. This flexure of the Gared rim was modeled with the ANSYS 2025R1 [22] Workbench modal analysis system, using 1827 TET10 elements. The TET10 element is a parabolic, three-dimensional, tetrahedral element with ten nodes, comprising four corner nodes and six mid-side notes. Build-tree steps 1-22 described in Winarski, et-al., [23], were used to model the Gared rim.

 doi:10.20944/preprints202504.0177.v1

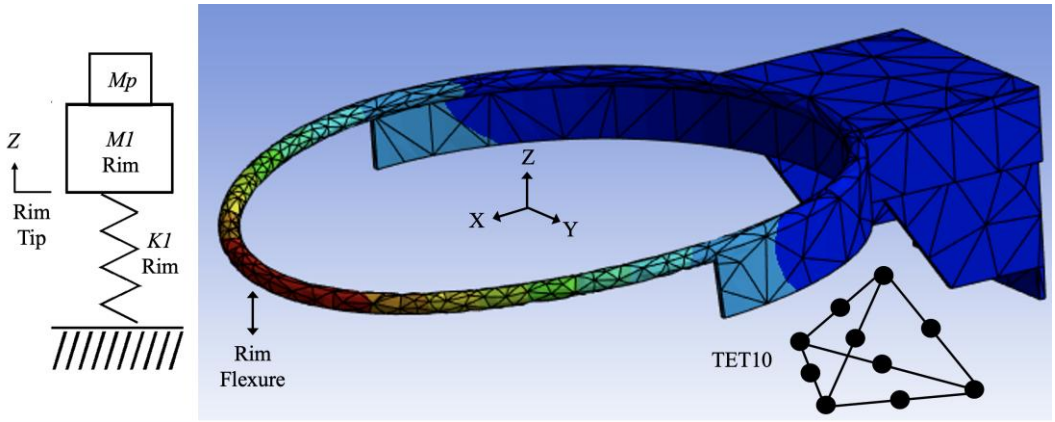

Figure 2. Spring-Mass and Finite-Element models of the flexure of one Gared rim.

Table 1 lists the empirical modal measurements of frequency and damping ratio for this Gared breakaway rim, first with no perturbation mass, then with the perturbation mass *Mp*. The damped frequency ω_d and damping ratio ζ in Table 1 were measured using the same Brüel & Kjær (B&K) 2034 signal analyzer, B&K 4393 accelerometer [21], B&K 8202 impact hammer [24], B&K 8200 force transducer, B&K 2644 line-driver charge-amplifiers [25], and Structural Measurements System (SMS) StarStruc software as used on the basketball rim and backboard, Winarski, et-al., [26]. The B&K 8202 impact hammer (excitation) was used to gently tap the rim, and the B&K 4393 accelerometer sensed the subsequent response. The outputs of the Brüel & Kjær (B&K) 2034 signal analyzer were Frequency Response Functions (*.FRF) which were Bode plots of amplitude versus frequency and phase angle versus frequency. Structural Measurements System (SMS) StarStruc software performed the calculation of frequency and damping ratios.

Table 1. Empirical modal measurements of one Gared rim in isolation.

Pertubation Mass *Mp*	Flexural Frequency ω_d	Damping Ratio ζ
0 kg (none)	40.25 Hz	0.19327%
0.5 kg	31.55 Hz	0.16007%

Table 2 lists the dynamic mass *M1*, damping *C1*, and spring rate *K1* calculated via these equations. First of all, the damping ratios in Table 1 were so low that the natural frequency ω of the spring-mass model was assumed to be equal to the damped natural frequency ω_d.

$$\omega = \frac{\omega d}{\sqrt{1-\zeta^2}} \approx \omega d$$

The first equation is for the natural frequency ω of the spring-mass system in Figure 2 without a perturbation mass. The second equation is for the perturbed natural frequency ωp spring-mass system augmented with a known perturbation mass, *Mp*.

$$\omega = 40.25\text{Hz} = \sqrt{K1/M1}$$
$$\omega p = 31.55\text{Hz} = \sqrt{K1/(M1+Mp)}$$

The following ratio was created from the above two equations, where spring-rate *K1* was eliminated. Table 1 lists the natural frequency ω = 40.25Hz without a perturbation mass, followed by the perturbed natural frequency ωp = 31.55Hz caused by the perturbation mass *Mp* = 0.5kg. Solving for the dynamic mass of the rim gave, *M1* = 0.797kg, as shown in Table 2.

$$\omega/\omega p = 40.25/31.55 = \sqrt{(M1+0.5)/M1}$$

The value of the dynamic mass of the rim, *M1*, allowed calculation of *K1* = *M1*×$(2\pi\omega)^2$ = 50,960 N/m, as shown in Table 2. The critical damping was calculated as Cc = $2\sqrt{K1 \times M1}$ = 403 Ns/m. This gave a value of damping C1=ζ×Cc=0.0019327×403 = 0.779 Ns/m, as shown in Table 2.

Preprints.org (www.preprints.org) | NOT PEER-REVIEWED | Posted: 2 April 2025 doi:10.20944/preprints202504.0177.v1

Table 2. Dynamic Mass, Damping, and Spring Rate of one Gared rim in isolation.

Dynamic Mass *M1*	Damping *C1*	Spring Rate *K1*
0.797 kg	0.779 Ns/m	50,960 N/m

The ratio ω/ωp = 40.25/31.55 = 1.276 was calculated from the empirical modal analysis, Table 1. The same ratio ω/ωp of 1.276 was obtained from ANSYS finite element modeling. A point mass of 0.5kg was used to model the perturbation mass *Mp* = 0.5kg in ANSYS.

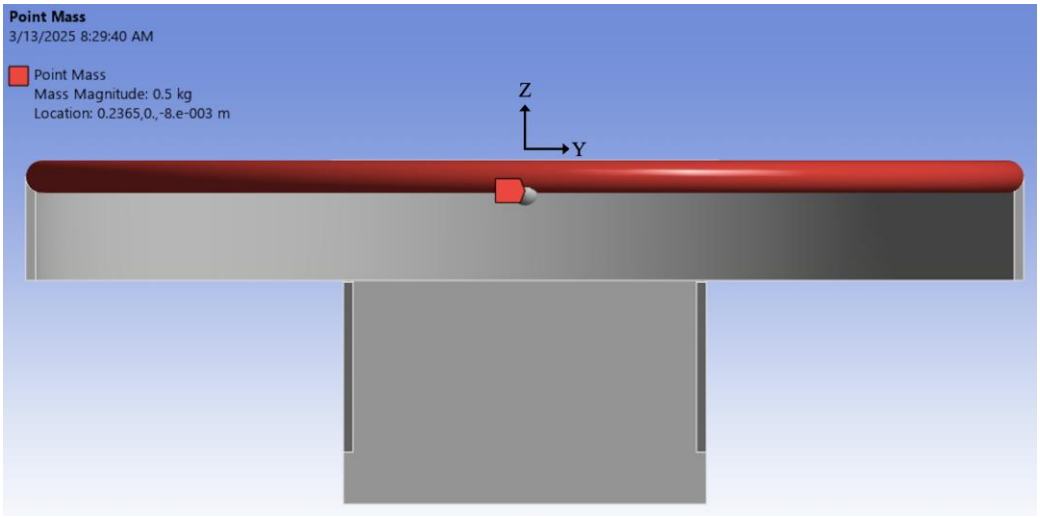

Figure 3. Point Mass of 0.5kg used to model the perturbation mass *Mp* in ANSYS.

After the completion of the quantification of the Gared rim, an A12N basketball was included.

3. Gared Rim and A12N Basketball

This section first determined the dynamic mass *M2* of an A12N basketball and its radial spring rate *K2* as a function of internal air pressure P. Then the sensitivity of the radial spring rate *K2* of the basketball versus air pressure investigated. Finally, the damping ratios ζ of the first and second modes of the combined A12N basketball and rim versus internal pressure P were calculated.

Table 3 lists the empirical modal measurements of the first two modes of vibration of the combined Gared rim, previously quantified in Table 2, and an A12N basketball. The same empirical modal analysis methods used to study the Gared rim in isolation were used to study the Gared rim and A12N basketball in combination. The A12N basketball was inflated to two air pressures, 68.94kPa and 34.47kPa. Two added masses *Ma* atop the basketball were used to engage the A12N basketball with the rim. These were 0.4kg and 0.8kg, each with an added 65.8g mass to account for a light stabilizing beam which exerted just enough force to hold the A12N basketball in place.

Table 3. Empirical measurements of first two modes of Gared rim and A12N basketball.

A12N Ball Pressure	Added Mass *Ma*	Mode-1 ω_d Frequency	Mode-1 ζ Damping Ratio	Mode-2 ω_d Frequency	Mode-2 ζ Damping Ratio
68.94 kPa	0.4658 kg	18.88 Hz	2.72%	49.65 Hz	1.48%
34.47 kPa	0.4658 kg	17.73 Hz	4.07%	47.63 Hz	2.29%
68.94 kPa	0.8658 kg	16.43 Hz	2.25%	49.21 Hz	1.52%
34.47 kPa	0.8658 kg	15.07 Hz	3.58%	47.34 Hz	1.84%

Using the lumped-parameter model shown in Figure 4, the mass matrix [*M*] for this two degree-of-freedom analysis was given as:

$$Mass\ Matrix = [M] = \begin{bmatrix} M1 & 0 \\ 0 & M2 + Ma \end{bmatrix}$$

The symmetric spring matrix [*K*] was given as:

Preprints.org (www.preprints.org) | NOT PEER-REVIEWED | Posted: 2 April 2025 doi:10.20944/preprints202504.0177.v1

$$Spring\ Matrix = [K] = \begin{bmatrix} K1+K2 & -K2 \\ -K2 & K2 \end{bmatrix}$$

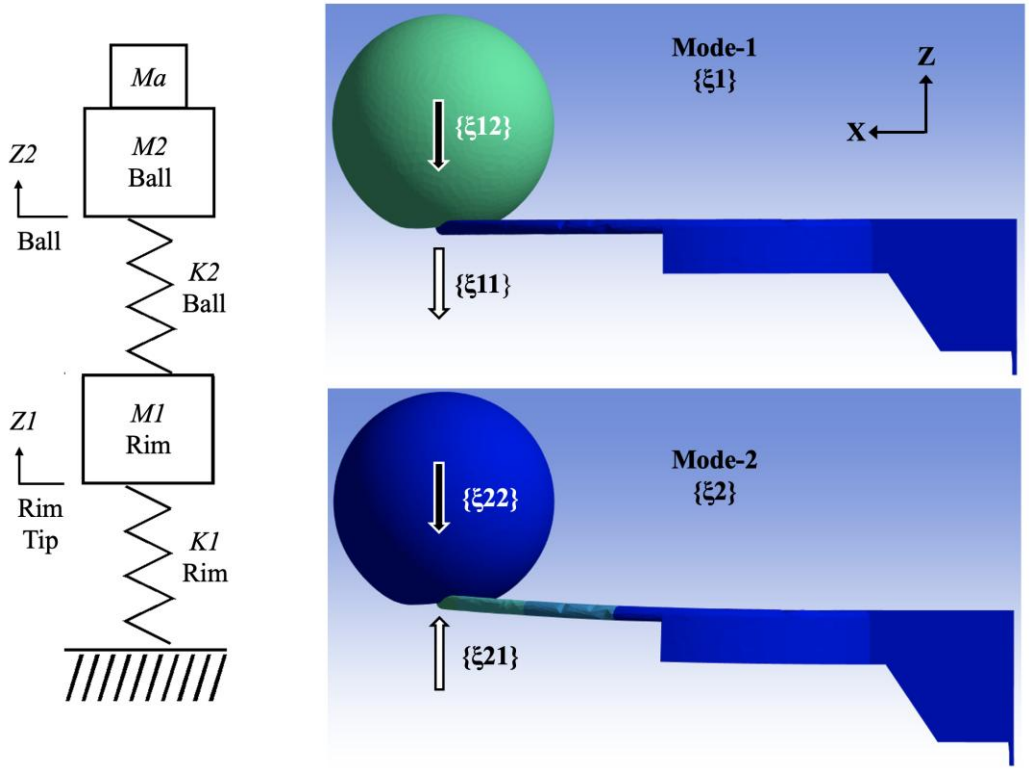

Figure 4. Lumped-Parameter and ANSYS models of Rim-Ball Interaction.

To evaluate the eigenvalues λ of this two degree-of-freedom system, the determinant of $[M]^{-1}[K] - \lambda[I]$ was set to zero to produce a quadratic characteristic equation with two solutions.

$$det\begin{bmatrix} \frac{K1+K2}{M1} - \lambda & -\frac{K2}{M1} \\ -\frac{K2}{M2+Ma} & \frac{K2}{M2+Ma} - \lambda \end{bmatrix} = 0$$

The following two equations were derived from the above determinant. In these equations, $\lambda 1$ was associated with mode 1, and $\lambda 2$ was associated with mode 2, in Table 3.

$$\lambda 2 + \lambda 1 = \frac{K1+K2}{M1} + \frac{K2}{M2+Ma}$$

$$(\lambda 2 - \lambda 1)^2 = (\lambda 2 + \lambda 1)^2 - \frac{4 \times K1 \times K2}{M1 \times (M2+Ma)}$$

These two equations can be combined to eliminate (*M2*+*Ma*), thus giving one equation and one unknown, namely the radial spring rate of the A12N basketball, *K2*.

$$(\lambda 2 - \lambda 1)^2 = (\lambda 2 + \lambda 1)^2 - \frac{4 \times K1}{M1} \times \left[(\lambda 2 + \lambda 1) - \frac{K1+K2}{M1}\right]$$

$$K2 = M1 \times \left[(\lambda 2 + \lambda 1) - \frac{M1}{4 \times K1}[(\lambda 2 + \lambda 1)^2 - (\lambda 2 - \lambda 1)^2]\right] - K1$$

$$K2 = M1 \times \left[(\lambda 2 + \lambda 1) - \frac{M1 \times \lambda 1 \times \lambda 2}{K1}\right] - K1$$

Once the radial spring rate of the basketball, *K2*, was identified, the equation for the dynamic mass of the basketball *M2* was given as:

$$M2 = \frac{K2}{(\lambda 2 + \lambda 1) - \frac{K1+K2}{M1}} - Ma$$

Table 4 lists the calculated dynamic mass *M2* and dynamic spring rate *K2* of the A12N basketball. The 22 ounce (0.62kg) specified dead-weight mass of the men's NCAA size-7 basketball [18] was surprisingly close to its slightly smaller dynamic mass *M2*≈0.5kg. The circumference of the basketball was specified at 29.5 inches (749mm).

 doi:10.20944/preprints202504.0177.v1

Table 4. Empirical Mode Frequencies and Eigenvalues, Ball Mass and Spring Rate.

A12N Ball Pressure	Added Mass *Ma*	Mode-1 Frequency	Mode-2 Frequency	Mode-1 $\lambda 1$ Eigenvalue	Mode-2 $\lambda 2$ Eigenvalue	Ball Mass *M2*	Ball Spring Rate *K2*
68.94 kPa	0.4658 kg	18.88 Hz	49.65 Hz	14072.2 s^{-2}	97319.0 s^{-2}	0.503 kg	20,748 N/m
34.47 kPa	0.4658 kg	17.73 Hz	47.63 Hz	12410.1 s^{-2}	89561.3 s^{-2}	0.481 kg	16,457 N/m
68.94 kPa	0.8658 kg	16.43 Hz	49.21 Hz	10657.0 s^{-2}	95601.7 s^{-2}	0.454 kg	21,029 N/m
34.47 kPa	0.8658 kg	15.07 Hz	47.34 Hz	8965.73 s^{-2}	88474.0 s^{-2}	0.489 kg	16,812 N/m

The eigenvectors {ξ} associated with the first two modes of vibration were very interesting and were derived using the following maxtrix equation. To compare these eigenvectors with Figure 4, the parameters in Tables 3 and 4 were used.

$$\begin{bmatrix} (K1+K2)/M1 - \lambda & -K2/M1 \\ -K2/(M2+Ma) & K2/(M2+Ma) - \lambda \end{bmatrix} \{\xi\} = 0$$

Using the first row of Table 4, where the ball pressure was 68.94 kPa and the added mass was 0.4658kg, the eigenvalue calculated for the first mode was $\lambda 1$ = 14072.2 radians²/second². With *K1*, *M1*, *K2*, and *M2* defined in Tables 3 and 4, the matrix equation for the first orthonormal eigenvector {ξ1} became:

$\begin{bmatrix} 75900.2 & -26032.6 \\ -21416.2 & 7344.0 \end{bmatrix} \{\xi 1\} = 0$, the solution of which was $\{\xi 1\} = \begin{Bmatrix} 0.2641 \\ 0.9459 \end{Bmatrix}$.

Thus, the calculated orthonormal eigenvector {ξ1} for mode-1 showed the motion of the rim and A12N basketball to be in-phase, exactly as shown in Figure 4, with both eigenvector arrows both pointing down in that figure for mode-1. This eigenvector {ξ1} for mode-1 also indicated that there is more motion associated with the A12N basketball than the Gared rim, which was also the case for the ANSYS finite element model.

The ANSYS finite element model for the basketball in Figure 4 was created with via a primitive thin-shell sphere, which used 6955 TET10 elements. This was the same type of element used to model the rim, Figure 2. This gave 8782 TET10 elements overall, 1827 for the rim and 6955 basketball, as shown in Table 5.

Table 5. Elements and Nodes used in ANSYS Finite Element Analysis.

Component	TET10 Elements	Nodes	Corner Nodes	Mid Nodes
Gared Rim	1827	3861	685	3176
A12N Basketball	6955	14053	2374	11679
Total	8782	17914	3059	14855

The eigenvalue calculated for the second mode was $\lambda 2$ = 97319.0 radians²/second². The matrix equation for the second orthonormal eigenvector {ξ2} became:

$\begin{bmatrix} -7346.6 & -26032.6 \\ -21416.2 & -75902.8 \end{bmatrix} \{\xi 2\} = 0$, the solution of which $\{\xi 2\} = \begin{Bmatrix} 0.9624 \\ -0.2716 \end{Bmatrix}$.

Thus, the calculated eigenvector {ξ2} for mode-2 showed the motion of the rim and A12N basketball to be 180° out of phase, exactly as shown in Figure 4. This orthonormal eigenvector {ξ2} for mode-2 also indicated that there is more motion associated with the Gared rim than the A12N basktball, which was also the case for the ANSYS finite element model.

These two orthonormal eigenvectors {ξ1} = {ξ11 ξ12}^{T} and {ξ2} = {ξ21 ξ22}^{T} were then checked for orthogonality using the equation {ξ1}^{T}[M]{ξ2}=0.

$$\{\xi 11 \;\; \xi 12\} \begin{bmatrix} M1 & 0 \\ 0 & M2+Ma \end{bmatrix} \begin{Bmatrix} \xi 21 \\ \xi 22 \end{Bmatrix} = 0$$

The above equation gave ξ11×*M1*×ξ21 + ξ12×(*M2*+*Ma*)×ξ22 = 0. Inserting information from the top row of Table 6 gave 0.2641×0.797×0.9624 − 0.9459×(0.503+0.4658)×0.2716 = 0.0, which shows that this set of eigenvectors associated with the Gared rim, and the A12N basketball with an internal pressure P=68.94kPa and an additional mass *Ma*=0.4658kg, were indeed orthogonal.

 doi:10.20944/preprints202504.0177.v1

The values of {ξ1} for mode-1 and {ξ2} for mode-2 were listed in Table 6 for both inflation pressures P and both added masses *Ma*. The check for orthogonality, $\{\xi 1\}^T[M]\{\xi 2\}$, was also included in Table 6.

Table 6. Orthonormal Eigenvectors {ξ1} for Mode-1 and {ξ2} for Mode-2.

A12N Ball Pressure P	Added Mass *Ma*	Mode-1 {ξ1} Eigenvector	Mode-2 {ξ2} Eigenvalue	$\{\xi 1\}^T[M]\{\xi 2\}$
68.94 kPa	0.4658 kg	$\{0.2641, 0.9459\}^T$	$\{0.9624, -0.2716\}^T$	0.0
34.47 kPa	0.4658 kg	$\{0.2282, 0.9614\}^T$	$\{0.9722, -0.2341\}^T$	0.0
68.94 kPa	0.8658 kg	$\{0.2569, 0.9493\}^T$	$\{0.9806, -0.1961\}^T$	0.0
34.47 kPa	0.8658 kg	$\{0.2224, 0.9636\}^T$	$\{0.9869, -0.1609\}^T$	0.0

Figure 5 depicts the rotation of the eigenvectors due to change of inflation pressure P, using the information from the first two rows of Table 6, where the added mass *Ma* was 0.4658kg.

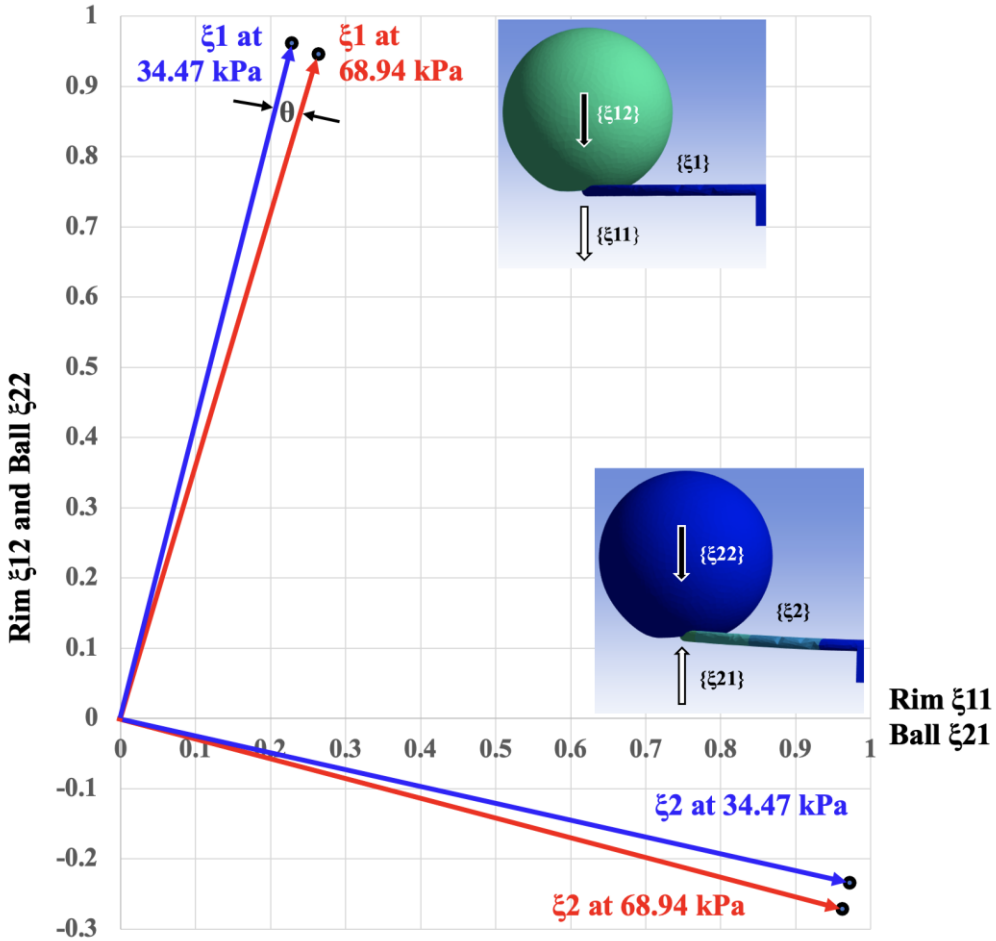

Figure 5. Rotation angle θ of Eigenvectors as a function of Basketball Pressure P.

Figure 5 shows a 39.3 milliradian (2.25 degrees) clockwise rotation of orthonormal eigenvectors {ξ1} for Mode-1 and {ξ2} for Mode-2 as the inflation pressure P was increased from 34.47kPa to 68.94kPa. Figure 5 provides a visual depiction of the physics of increased inflation pressure. As indicated in the first two rows of Table 6, as inflation pressure increases from 34.47kPa to 68.94kPa, the magnitude of ξ11 increases from 0.2282 to 0.2641 while the magnitude of ξ12 decreases from 0.9614 to 0.9459. Simulateously, the magnitude of ξ21 decreases from 0.9722 to 0.9624 while the magnitude of ξ22 shifts from -0.2341 to -0.2716. The net result is that the pair of orthonormal eigenvectors {ξ1} for Mode-1 and {ξ2} for Mode-2 rotates clockwise.

 doi:10.20944/preprints202504.0177.v1

When the added mass mass *Ma* was 0.8658kg, the bottom two rows of Table 6, a similar 37.4 milliradian (2.14 degrees) clockwise rotation of orthonormal eigenvectors {ξ1} for Mode-1 and {ξ2} for Mode-2 was calculated, as the inflation pressure P was increased from 34.47kPa to 68.94kPa. The series by Davis, et-al., "The Rotation of Eigenvectors by a Perturbation," [27-29], was helpful in understanding the perturbation-induced rotations of eigenvectors in Figure 5 and Table 6.

4. Variation of Radial Spring Rate and Damping Ratio of A12N Basketball versus Pressure

In Table 7, the variation of the radial spring rate *K2* of the A12N basketball versus internal pressure P was calculated as $\Delta K2/\Delta P$. The statistical cross-correlation between radial spring rate *K2* of the A12N basketball versus internal pressure P was calculated at 99.72%, with 100% representing a perfect direct correlation. The =PEARSON function in Excel was used to calculate this cross-correlation. The units of $\Delta K2/\Delta P$ were N/m divided by N/m² (Pascals) which simplified to meters m. $\Delta K2/\Delta P>0$ indicated that the higher the internal pressure P, the stiffer the basketball.

The statistical cross-correlation between the radial spring rate *K2* of the A12N basketball versus added mass *Ma* was calculated at 7.45%, with 0% representing no correlation at all. Thus, the added mass *Ma* had no meaningful effect on the radial spring rate of the A12N basketball, as evidenced by $\Delta K2/\Delta P$=0.124m for *Ma*=0.4658kg and $\Delta K2/\Delta P$=0.122m for Ma=0.8658kg.

Table 7. Variation of Basketball Radial Spring Rate *K2* with respect to Ball Pressure.

Added Mass *Ma*	A12N Ball Pressure P	Ball Spring Rate *K2*	A12N Ball Pressure P	Ball Spring Rate *K2*	$\Delta K2/\Delta P$
0.4658 kg	68.94 kPa	20,748 N/m	34.47 kPa	16,457 N/m	0.124 m
0.8658 kg	68.94 kPa	21,029 N/m	34.47 kPa	16,812 N/m	0.122 m

In Table 8, the variation of the damping ratios ζ of the first and second modes of the combined A12N basketball and Gared rim versus internal pressure P were calculated as $\Delta\zeta/\Delta P$. The statistical cross-correlation between damping ratios ζ of the first two modes of vibration of the A12N basketball and rim versus internal pressure P was calculated at -94.14% for the first mode of vibration and a -87.05% for the second mode of vibration, with -100% representing a perfect inverse correlation. $\Delta\zeta/\Delta P<0$ in all cases, indicating that the higher the internal pressure P, the lower the damping ratios of the first two modes of vibration of the A12N basketball and Gared rim.

Table 8. Variation of Basketball-Rim Damping Ratios ζ with respect to Ball Pressure P.

Added Mass *Ma*	Mode	A12N Ball Pressure P	Damping Ratio ζ	A12N Ball Pressure P	Damping Ratio ζ	$\Delta\zeta/\Delta P$
0.4658 kg	1	68.94 kPa	2.72%	34.47 kPa	4.07%	-0.0392 %/kPa
0.4658 kg	2	68.94 kPa	1.48%	34.47 kPa	2.29%	-0.0235 %/kPa
0.8658 kg	1	68.94 kPa	2.25%	34.47 kPa	3.58%	-0.0386 %/kPa
0.8658 kg	2	68.94 kPa	1.52%	34.47 kPa	1.84%	-0.0093 %/kPa

5. Conclusions

Our hypothesis was confirmed, namely that the radial spring rate *K2* of the basketball would have a high positive correlation and the damping ratios of the first two modes of vibration of the basketball and rim would have a high negative correlation with respect to the inflation pressure P. The statistical cross-correlation between radial spring rate of the basketball versus internal pressure P was calculated at 99.72%, with 100% representing a perfect direct correlation. The statistical cross-correlation between damping ratios ζ of the first two modes of vibration of the basketball and rim versus internal pressure P was calculated at -94.14% for the first mode of vibration and a -87.05% for

 doi:10.20944/preprints202504.0177.v1

the second mode of vibration, with -100% representing a perfect inverse correlation. We found that $\Delta K2/\Delta P>0$ and $\Delta\zeta/\Delta P<0$ in all cases, reinforcing our correlations.

We also found that the diagram of the rotation of the eigenvectors of our basketball-rim system was very instructive in explaining the changes in the modes of vibration versus inflation pressure P.

There is a limitation to the basketball-rim modeling presented in this study. There are many possible designs of rims which meet NCAA standards. This study only involved one basketball rim, so this study is currently not comprehensive across the entire sport of basketball.

Author Contributions: Conceptualization, K.P.N.; methodology, D.W.; validation, K.P.N., D.W. and T.W.; formal analysis, D.W. and T.W.; investigation, D.W. and T.W.; writing—original draft preparation, D.W.; writing—review and editing, K.P.N., D.W. and T.W.; visualization, K.P.N. and D.W.; supervision, K.P.N.; project administration, K.P.N. All authors have read and agreed to the published version of the manuscript.

Funding: This research received no external funding.

Acknowledgments: Ms. Donna Robinson Winarski is acknowledged for her support of this research, both at the United States Military Academy at West Point, New York, and at Tucson, Arizona. Her assistance with initial editing as well as data taking was very much appreciated.

Conflicts of Interest: The authors declare no conflict of interest.

Abbreviations

The following abbreviations were used in this manuscript:

[K]	Spring Matrix
K1	Dynamic Spring Rate of the Gared Rim, N/m
K2	Dynamic Radial Spring Rate of the A12N Basketball, N/m
[M]	Mass Matrix
M1	Dynamic Mass of the Gared Rim, kg
M2	Dynamic Mass of the A12N Basketball, kg
Ma	Added Mass to top of A12N Basketball, kg
Mp	Perturbation Mass added to Gared Rim, kg
P	Inflation Pressure of A12N Basketball, kPa
λ	Eigenvalue, square of natural frequency, radians^2/second^2
{Ξ1}	Orthonormal Eigenvector, describing vibration directions of mode-1
{Ξ2}	Orthonormal Eigenvector, describing vibration directions of mode-2
ζ	Damping Ratio
θ	Rotation angle of Eigenvectors due to Inflation Pressure P, milliradians
ω	Natural Frequency, Hertz
ω_d	Damped Natural Frequency, Hertz

References

1. Okubo, Hiroki, *and* Mont Hubbard. "Identification of basketball parameters for a simulation model." *Procedia Engineering* 2, no. 2 (2010): 3281-3286. https://doi.org/10.1016/j.proeng.2010.04.145. (accessed on 28 March 2025).
2. Okubo, H., Hubbard, M. Dynamics of basketball-rim interactions. *Sports Eng* **7**, 15–29 (2004). https://doi.org/10.1007/BF02843970 (accessed on 28 March 2025).
3. Okubo, H., and M. Hubbard. "Dynamics of the basketball shot with application to the free throw." *Journal of sports sciences* 24, no. 12 (2006): 1303-1314. https://doi.org/10.1080/02640410500520401. (accessed on 28 March 2025).
4. Okubo, Hiroki, and Mont Hubbard. "Rebounds of basketball field shots." *Sports Engineering* 18 (2015): 43-54. (accessed on 28 March 2025).
5. Okubo, Hiroki, and Mont Hubbard. "Analysis of Arm Joint Torques at Ball-Release for Set and Jump Shots in Basketball." In *Proceedings*, vol. 49, no. 1, p. 4. MDPI, **2020**. https://doi.org/10.3390/proceedings2020049004. (accessed on 28 March 2025).

 doi:10.20944/preprints202504.0177.v1

6. Okubo, Hiroki, and Mont Hubbard. "Kinematic differences between set-and jump-shot motions in basketball." In *Proceedings*, vol. 2, no. 6, p. 201. MDPI, **2018**. https://doi.org/10.3390/proceedings2060201. (accessed on 28 March 2025).
7. Tanaka: K.; Sekizawa, K. Construction of a finite element model of golf clubs and influence of shaft stiffness on its dynamic behavior. *Proceedings* **2018**, *2*, 247.
8. Matsuda, A.; Nakui, M.; Hashiguchi, T. Simulation of Mechanical Characteristics of Tennis Racket String Bed Considering String Pattern. *Proceedings* **2018**, *2*, 264.
9. Takizawa, M.; Matsuda, A.; Hashiguchi, T. A Study on the Mechanical Characteristics of String Planes of Badminton Racquets by Nonlinear Finite Element Analysis. *Proceedings* **2020**, *49*, 42.
10. Yin, S.-R.; Chang, H.-C.; Cheng, K.B. Impact Characteristics of a Badminton Racket with Realistic Finite Element Modeling. *Proceedings* **2020**, *49*, 106.
11. Javorski, M.; Čermelj, P.; Boltežar, M. Characterization of the Dynamic Behaviour of a Basketball Goal Mounted on a Ceiling. *J. Mech. Eng./Stroj. Vestn.* **2010**, *56*. Available online: https://www.sv-jme.eu/?ns_articles_pdf=/ns_articles/files/ojs3/1513/submission/1513-1-2001-1-2-20171103.pdf&id=5958 (accessed on 9 September 2023).
12. Nkounhawa, Pascal Kuate, et al. "Analysis of the Behavior of a Square Plate in Free Vibration by FEM in Ansys." *World Journal of Mechanics* 10.02 (2020): 11-25.
13. Guguloth, Ganesh Naik, Baij Nath Singh, and Vinayak Ranjan. "Free vibration analysis of simply supported rectangular plates." *Vibroengineering Procedia* 29 (2019): 270-273.
14. Irvine, T. The Natural Frequency of a Rectangular Plate Point-Supported at Each Corner, Revision C. 1 August 2011. Available online: http://www.vibrationdata.com/tutorials2/plate_point_corner.pdf (accessed on 25 July 2023).
15. Dumond, P.; Monette, D.; Alladkani, F.; Akl, J.; Chikhaoui, I. Simplified setup for the vibration study of plates with simply- supported boundary conditions. *Methods X* **2019**, *6*, 2106–2117.
16. Anđelić, N., M. Čanađija, and Z. Car. "Determination of Natural Vibrations of Simply Supported Single Layer Graphene Sheet using Non-Local Kirchhoff Plate Theory." *IN-TECH 2017 International Conference on Innovative Technologies*. 2017, p.5.
17. Geveci, Berk, and J. D. A. Walker. "Nonlinear resonance of rectangular plates." *Proceedings of the Royal Society of London. Series A: Mathematical, Physical and Engineering Sciences* 457.2009 (2001): 1215-1240.
18. Covill, D.; Drouet, J.-M. On the Effects of Tube Butting on the Structural Performance of Steel Bicycle Frames. *Proceedings* **2018**, *2*, 216.
19. Model 3500 Positive Lock Breakaway Goal. Updated 21 January 2010. Gared Holdings, LLC. Available online: https://www. garedsports.com/sites/default/files/import/files/3500I%2520spec%2520-revA.pdf (accessed on 7 September 2023).
20. 2024-2025 NCAA Men's Basketball Rules Handbook, August 2024. Manuscript Prepared By: Jeff O'Malley, Secretary-Rules Editor, NCAA Men's Basketball Rules Committee. Edited By: Andy Supergan, Associate Director of Playing Rules and Officiating. https://www.ncaapublications.com/productdownloads/BK25.pdf (accessed on 13 November 2024).
21. *Product Data: Piezoelectric Charge Accelerometer Types 4393 and 4393-V*. Copyright 2018-08 by Brüel & Kjaer. Downloaded from: https://www.bksv.com/media/doc/bp2043.pdf (accessed on 30 July 2023).
22. ANSYS 2025 R1 Student Edition: Available online: https://www.ansys.com/academic/students/ansys-student (accessed on 15 February 2025).
23. Winarski, Daniel, Kip P. Nygren, and Tyson Winarski. 2024. "Finite Element Analysis versus Empirical Modal Analysis of a Basketball Rim and Backboard" *Vibration* 7, no. 2: 582-594. https://doi.org/10.3390/vibration7020030. Available online at https://www.mdpi.com/2571-631X/7/2/30.
24. Technical Documentation: Impact Hammer Type 8202. Copyright May, 1993 by Brüel & Kjaer. Available online: https://media. hbkworld.com/m/7a8ee3f9bea9db2b/original/Impact-Hammer-Type-8202.pdf (accessed on 30 July 2023).
25. Serridge, M.; Licht, T. *Piezoelectric Accelerometers and Vibration Preamplifiers: Theory and Application Handbook*; Brüel & Kjær: Naerum, Denmark, 1987. Available online: https://www.bksv.com/media/doc/bb0694.pdf (accessed on 30 July 2023).

 doi:10.20944/preprints202504.0177.v1

26. Winarski, Daniel, Kip P. Nygren, and Tyson Winarski. 2023. "Modes of Vibration in Basketball Rims and Backboards and the Energy Rebound Testing Device" *Vibration* 6, no. 4: 726-742. https://doi.org/10.3390/vibration6040045. Available online: https://www.mdpi.com/2571-631X/6/4/45.
27. Davis, Chandler. "The rotation of eigenvectors by a perturbation." *Journal of Mathematical Analysis and Applications (US)* 6 (1963). (accessed on 31 March 2025).
28. Davis, Chandler. "The rotation of eigenvectors by a perturbation. II." *J. Math. Anal. Appl* 11, no. 2 (1965): 27. (accessed on 1 April 2025).
29. Davis, Chandler, and William Morton Kahan. "The rotation of eigenvectors by a perturbation. III." *SIAM Journal on Numerical Analysis* 7, no. 1 (1970): 1-46. (accessed on 1 April 2025).